

## Infrared probe of the insulator-to-metal transition in $\text{Ga}_{1-x}\text{Mn}_x\text{As}$ and $\text{Ga}_{1-x}\text{Be}_x\text{As}$

B. C. Chapler,<sup>1,\*</sup> R. C. Myers,<sup>2</sup> S. Mack,<sup>3</sup> A. Frenzel,<sup>1</sup> B. C. Pursley,<sup>1</sup> K. S. Burch,<sup>4</sup> E. J. Singley,<sup>5</sup>  
A. M. Dattelbaum,<sup>6</sup> N. Samarth,<sup>7</sup> D. D. Awschalom,<sup>3</sup> and D. N. Basov<sup>1</sup>

<sup>1</sup>*Physics Department, University of California-San Diego, La Jolla, California 92093, USA*

<sup>2</sup>*Department of Materials Science and Engineering, Ohio State University, Columbus, Ohio 43210, USA*

<sup>3</sup>*Center for Spintronics and Quantum Computation, University of California-Santa Barbara, California 93106, USA*

<sup>4</sup>*Department of Physics & Institute for Optical Sciences, University of Toronto, Toronto, Ontario, Canada M5S 1A7*

<sup>5</sup>*Department of Physics, California State University-East Bay, Hayward, California 94542, USA*

<sup>6</sup>*Los Alamos National Laboratory, Los Alamos, New Mexico 87545, USA*

<sup>7</sup>*Department of Physics, The Pennsylvania State University, University Park, Pennsylvania 16802, USA*

(Received 18 July 2011; published 26 August 2011)

We report infrared studies of the insulator-to-metal transition (IMT) in GaAs doped with either magnetic (Mn) or nonmagnetic acceptors (Be). We observe a resonance with a natural assignment to impurity states in the insulating regime of  $\text{Ga}_{1-x}\text{Mn}_x\text{As}$ , which persists across the IMT to the highest doping (16%). Beyond the IMT boundary, behavior combining insulating and metallic trends also persists to the highest Mn doping. Be-doped samples, however, display conventional metallicity just above the critical IMT concentration, with features indicative of transport within the host valence band.

DOI: [10.1103/PhysRevB.84.081203](https://doi.org/10.1103/PhysRevB.84.081203)

PACS number(s): 78.66.Fd, 71.30.+h, 73.50.-h, 75.50.Pp

The insulator-to-metal transition (IMT) becomes exceptionally complex when magnetism is involved, as proven in materials such as mixed-valence manganites, rare-earth chalcogenides, and Mn-doped III-V compounds.<sup>1-3</sup> In all these systems, the electronic and magnetic properties are typically interconnected, creating a challenge to understand how magnetism affects the IMT physics. A promising route to isolate differences attributable to the presence of magnetism on the IMT physics is to investigate either magnetic or nonmagnetic dopants in the same host. *p*-doped GaAs is well suited for the task since metallicity in this material can be initiated by nonmagnetic (Zn, Be, C) and magnetic (Mn) acceptors. Infrared (IR) experiments reported here for  $\text{Ga}_{1-x}\text{Be}_x\text{As}$  and  $\text{Ga}_{1-x}\text{Mn}_x\text{As}$  monitor the charge dynamics and electronic structure in the course of the IMT. Our results establish that the onset of conduction in magnetically doped GaAs is distinct from genuine metallic behavior due to extended states in the host valence band (VB), as seen in moderately doped  $\text{Ga}_{1-x}\text{Be}_x\text{As}$ . Moreover, we observe a coexistence of “metallic” and “insulating” trends over a broad range of Mn concentrations (1%–16%), underscoring the unconventional nature of Mn-doped GaAs beyond the IMT boundary.

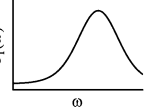
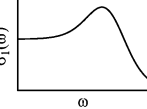
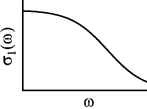
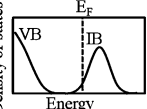
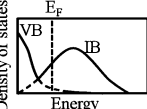
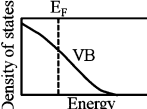
The  $\text{Ga}_{1-x}\text{Mn}_x\text{As}$  samples were prepared using a nonrotated, low-temperature, molecular-beam-epitaxy (MBE) technique, which has been shown to minimize the formation of compensating defects.<sup>4,5</sup> Several samples were also subjected to post-growth annealing in attempt to further reduce and eliminate defects. The IMT in  $\text{Ga}_{1-x}\text{Be}_x\text{As}$  occurs at significantly lower dopant concentration due to the much lower acceptor level [ $E_{\text{Be}} = 28$  meV,  $E_{\text{Mn}} = 112$  meV (Ref. 6)], thus samples near the  $\text{Ga}_{1-x}\text{Be}_x\text{As}$  IMT were grown using conventional equilibrium MBE. Importantly, the most metallic  $\text{Ga}_{1-x}\text{Be}_x\text{As}$  sample,  $\text{Ga}_{0.991}\text{Be}_{0.009}\text{As}$ , was grown under the same nonrotated, low-temperature conditions as the  $\text{Ga}_{1-x}\text{Mn}_x\text{As}$  samples. We can therefore expect nominally similar levels of disorder as that of  $\text{Ga}_{1-x}\text{Mn}_x\text{As}$  samples

with  $x \sim 0.01$ . Details on sample growth can be found in the Supplemental Material.<sup>7</sup>

Through a combination of transmission and ellipsometric measurements, we have probed the optical properties of the samples over a broad range of frequencies, spanning  $\sim 40\text{--}40\,000$   $\text{cm}^{-1}$  (experimental details can be found in the Supplemental Material<sup>7</sup>). Here we primarily focus on the real (or dissipative) part of the optical conductivity [ $\sigma_1(\omega)$ ] from THz to just below the GaAs band-gap energy ( $\sim 40\text{--}10\,000$   $\text{cm}^{-1}$ ). Through this probe, signatures of three distinct electronic transport regimes in *p*-doped GaAs are revealed (see Table I): a regime of insulating behavior, a regime of genuine metallic behavior (i.e., no signs of thermal activation) due to extended states in a partially unoccupied VB, and an unusual intermediate regime of conduction, exhibiting elements of both insulating and metallic transport. We refer to this latter regime as impurity band (IB) conduction, with this term used to describe the persistence of a resonance associated with VB-to-IB transitions beyond the onset of conduction.

We begin by discussing the insulating regime of  $\text{Ga}_{1-x}\text{Mn}_x\text{As}$ . Figure 1(a) depicts the spectra for a paramagnetic  $\text{Ga}_{0.995}\text{Mn}_{0.005}\text{As}$  sample. The dominant feature of these data is a broad mid-IR resonance, with peak frequency ( $\omega_0$ ) near  $1700$   $\text{cm}^{-1}$ . Room-temperature data show substantial spectral weight at far-IR frequencies [Fig. 1(a)]. However, far-IR weight is transferred to the mid-IR resonance as the sample is cooled, and “freezes out” at low temperature. Elimination of far-IR spectral weight unambiguously reveals the thermally activated nature of the electronic transport in this dilute regime. In Fig. 1(d), we plot the temperature dependence of the “infrared resistivity” [ $\rho_{\text{IR}} = 1/\sigma_1(40\text{ cm}^{-1})$ ]. The data in dilute Mn-doped samples ( $x = 0.005, 0.0075$ ) show the systematic increase in  $\rho_{\text{IR}}$  expected in the case of thermally activated transport, in support of the conclusion of variable-range hopping inferred from direct resistivity measurements.<sup>8</sup> The existence of a narrow impurity band is not in dispute in dilutely doped insulating samples,<sup>9,10</sup>

TABLE I. Summary of the three transport regimes uncovered for *p*-doped GaAs. Conductivity schematics in the insulating and impurity band conduction regimes highlight the resonance associated with valence band to impurity band transitions. This is contrasted by the conductivity schematic in the genuinely metallic regime that highlights the Drude response due to free carriers. We only list Mn and Be dopings reported in this study.

	Insulator	IB conduction	Genuine metal
$dp/dT$	$> 0$	mixed	$< 0$
Be (%)	0.0038	0.0095	0.032, 0.9
Mn (%)	0.5, 0.75	1.5 – 16	NA
Conductivity (schematic)			
Band structure (schematic)			

thus the observed mid-IR resonance in the vicinity of  $E_{Mn}$  in insulating samples can be naturally assigned to VB-to-IB transitions. We note that numerous probes report evidence of an IB in moderately doped  $Ga_{1-x}Mn_xAs$ .<sup>11–19</sup> However, our results on dilute Mn-doped samples are distinct in that they establish a mid-IR resonance in the insulating state.

Figures 1(b) and 1(c) show the spectra of the ferromagnetic  $Ga_{0.97}Mn_{0.03}As^*$  and  $Ga_{0.908}Mn_{0.092}As^*$  samples (\* denotes annealed), the highest conducting  $Ga_{1-x}Mn_xAs$  samples in

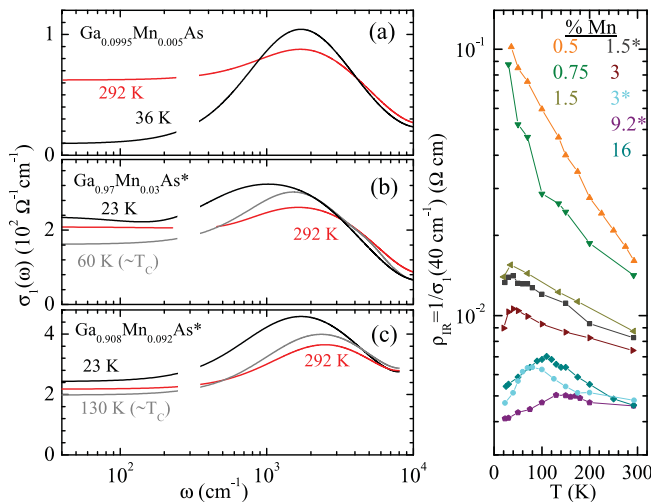


FIG. 1. (Color online) Characteristic spectra of the Mn-doped samples in the insulating (a) and IB conduction [(b) and (c)] regimes are exemplified by the  $Ga_{0.995}Mn_{0.005}As$ ,  $Ga_{0.97}Mn_{0.03}As^*$ , and  $Ga_{0.908}Mn_{0.092}As^*$  samples, respectively. The break in the spectra is due to a phonon in GaAs, which does not allow  $\sigma_1(\omega)$  to be extracted over this region. (d) The temperature dependence of  $\rho_{IR}$  for all Mn-doped samples in the study.

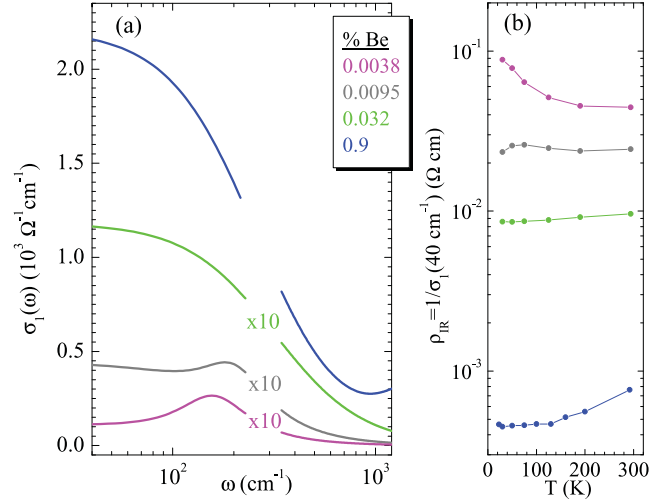


FIG. 2. (Color online) (a) Low-temperature ( $\sim 25$  K) spectra for the  $Ga_{1-x}Be_xAs$  samples. All spectra but that for the  $x = 0.009$  sample are multiplied by 10 to show on the same scale. (b) Temperature dependence of  $\rho_{IR}$  for all Be-doped samples.

this study. The spectra of both of these samples are characteristic of the IB conduction regime. The dominant feature of the spectra is a mid-IR resonance, similar in shape and  $\omega_0$  to the insulating sample. These samples additionally show a finite  $\sigma_{DC}$  in the limit of  $\omega, T \rightarrow 0$ : a condition often associated with the onset of metallicity. Nevertheless, a substantial fraction of the far-IR spectral weight still reveals activated behavior. Specifically, as the temperature is lowered from 300 K to near  $T_C$ , the far-IR spectral weight is suppressed and transferred to the mid-IR resonance, similar to data in Fig. 1(a).

The onset of ferromagnetism radically alters the temperature dependence of  $\sigma_1(\omega)$ . Below  $T_C$ , we observe the reversal of the activated character [black spectra in Figs. 1(b) and 1(c)], as the far-IR spectral weight, as well as the mid-IR resonance are enhanced. Earlier data have established a correlation between the enhancement of the spectral weight and the development of the magnetization.<sup>12</sup> Such enhancement serves as an unmistakable signature of the deep bond between magnetism and carrier dynamics in this class of carrier-mediated ferromagnets and other magnetic materials.<sup>1,20–22</sup> Comparison with dilute samples show the  $\rho_{IR}$  data still display (weakly) activated transport above  $T_C$ . Peaks in  $\rho_{IR}$  near  $T_C$  mark the reversal of activated trends.

Our data show the onset of conduction in  $Ga_{1-x}Mn_xAs$  occurs at a doping level  $0.0075 < x \leq 0.015$ , in excellent agreement with the Mott criterion ( $p_c^{1/3} = 2.78a_H$ , where  $p_c$  is the critical acceptor concentration and  $a_H$  is the effective Bohr radius of acceptor holes), corresponding to  $x = 0.0109$  for  $Ga_{1-x}Mn_xAs$  (assuming 1 hole/Mn and no compensation).<sup>6</sup> This agreement attests to a low degree of compensation in our samples, at least at doping regimes below a few atomic percent. We further note the IB conduction regime persists over an order of magnitude in dopant concentration, corresponding to at least  $x = 0.015–0.16$  in  $Ga_{1-x}Mn_xAs$ , as well as in heavily doped annealed samples ( $Ga_{0.908}Mn_{0.092}As^*$ ). No Mn-doped samples in this study were found to exhibit genuinely metallic behavior, which we report below for  $Ga_{1-x}Be_xAs$ .

Data in Fig. 2 display the IMT in  $\text{Ga}_{1-x}\text{Be}_x\text{As}$ . The  $x = 3.8 \times 10^{-5}$  and  $x = 9.5 \times 10^{-5}$  Be-doped samples (pink and gray curves in Fig. 2) reveal significant low-frequency conductivity at room temperature. However, the conductivity of the  $x = 3.8 \times 10^{-5}$  Be-doped sample is frozen out at low temperatures, analogous to the insulating  $\text{Ga}_{1-x}\text{Mn}_x\text{As}$  samples. Also similar to  $\text{Ga}_{1-x}\text{Mn}_x\text{As}$ , both  $x = 3.8 \times 10^{-5}$  and  $x = 9.5 \times 10^{-5}$  Be-doped samples show a resonance centered in the vicinity of the  $E_{\text{Be}}$ . Such a feature near the acceptor level reinforces a VB to dopant-induced IB interpretation in both Mn- and Be-doped GaAs. The  $\rho_{\text{IR}}$  data for the  $x = 9.5 \times 10^{-5}$  sample appear to show a finite  $\sigma_{\text{DC}}$  in the limit of  $\omega, T \rightarrow 0$ , implying this sample may be past the onset of conduction. Thus an intermediate IB conduction regime could be a generic feature of  $p$ -doped GaAs (and potentially many other doped semiconductors) near the IMT.<sup>23,24</sup>

Moving to the  $x = 3.2 \times 10^{-4}$  and  $x = 0.009$  Be-doped samples (light green and blue curves in Fig. 2), we see spectra qualitatively different from those observed in samples either in the insulating or IB conduction regimes. Here conductivity data are dominated by a pronounced Drude peak (Lorentzian centered at  $\omega = 0$ ), characteristic of delocalized carriers in a metal. Insights into the nature of the metallic state in  $\text{Ga}_{1-x}\text{Be}_x\text{As}$  is revealed by applying the partial sum rule to the conductivity

$$\int_0^{\omega_c} \sigma_1(\omega) d\omega = \frac{\pi p e^2}{2m_{\text{opt}}}. \quad (1)$$

This analysis yields the effective optical mass ( $m_{\text{opt}}$ ) provided the carrier density  $p$  is known. Using an integration cutoff of  $\omega_c = 6450 \text{ cm}^{-1}$ ,<sup>25</sup> we obtain  $m_{\text{opt}} = 0.28m_e$  and  $0.29m_e$  ( $m_e$  is the electron mass) for the  $x = 3.2 \times 10^{-4}$  and  $x = 0.009$  Be-doped samples, respectively. The extracted  $m_{\text{opt}}$  is in excellent agreement with calculations of the IR spectra of metallic  $p$ -doped GaAs with a partially unoccupied VB, which place  $m_{\text{opt}}$  between  $0.25m_e$  and  $0.29m_e$ .<sup>26</sup> These results, along with the metallic temperature dependence [green and blue curves in Fig. 2(b)], give strong evidence of transport due to light quasiparticles in a partially unoccupied VB. Note the Mott criterion for Be-doped GaAs predicts a critical dopant concentration of  $x = 2.7 \times 10^{-4}$ .<sup>6</sup> Thus our data indicate genuinely metallic behavior is achieved even for a 20% increase in dopant density beyond the Mott critical concentration. This latter finding stands in stark contrast to the case of Mn-doped samples.

To further highlight the differences between magnetic and nonmagnetic dopants in GaAs, we plot our results for the  $\text{Ga}_{1-x}\text{Mn}_x\text{As}$  samples, as well as the  $\text{Ga}_{0.991}\text{Be}_{0.009}\text{As}$  sample in Fig. 3(a). Figure 3(b) shows scaled conductivity for these samples, as well as earlier IR data for  $\text{Ga}_{1-x}\text{Mn}_x\text{As}$ , normalized by  $\sigma_1(\omega)$  at  $\omega_0$  along the y axis, and by  $\omega_0$  along the x axis. In both Mn- and Be-doped samples we observe a mid-IR resonance, however, a result that stands out in both panels is the difference in line shape of this resonance in genuinely metallic  $\text{Ga}_{1-x}\text{Be}_x\text{As}$  and that in the Mn-doped samples. The resonance seen in  $\text{Ga}_{0.991}\text{Be}_{0.009}\text{As}$  is much narrower and reveals a two-peak structure. The second peak appears as a shoulder on the main peak, and is most clearly seen near  $\omega/\omega_0 = 1.5$  in Fig. 3(b). The frequency position of the

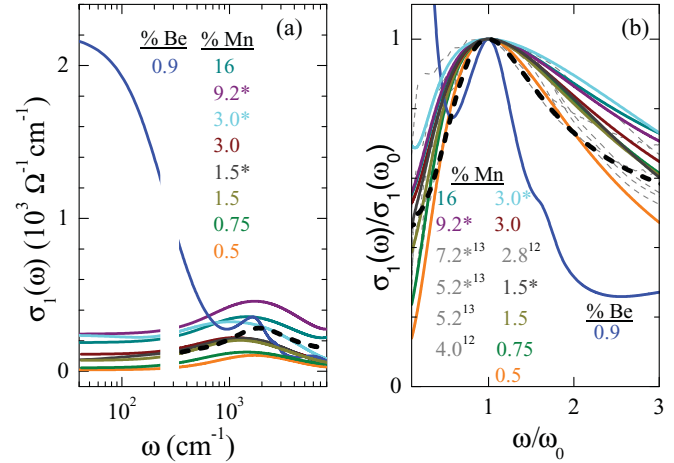


FIG. 3. (Color online) (a) Direct comparison of the conductivity spectra displayed for the lowest temperatures measured (20–36 K) of the  $x = 0.009$  Be-doped film and all Mn-doped films studied. (b) The mid-IR resonance in the two classes of materials is directly compared by normalizing spectra by the peak in  $\sigma_1(\omega)$  at  $\omega_0$  along the y axis, and by  $\omega_0$  along the x axis. Also shown in both panels is calculated  $\sigma_1(\omega)$  according to the quantum defect method (black dashed) (Ref. 14). Additional  $\text{Ga}_{1-x}\text{Mn}_x\text{As}$  data are reported from Burch *et al.* (Ref. 13) and Singley *et al.* (Ref. 12).

two-peak structure is an order of magnitude higher than  $E_{\text{Be}}$ , however, it is near the energy expected for intra-VB transitions, in accord with  $E_F$  located deep within the VB. The main peak is thus attributed light-hole band (LH) to heavy-hole band (HH) excitations,<sup>27</sup> while the shoulder is due to excitations from the split-off band (SO).<sup>28</sup>

In contrast to our observations in the  $\text{Ga}_{0.991}\text{Be}_{0.009}\text{As}$  film, all the Mn-doped samples (both in the insulating regime and those past the onset of conduction) show very broad, structureless absorption. Furthermore, upon scaling of these data [Fig. 3(b)], the Mn-doped samples reveal a nearly identical line shape, barring small nonmonotonic differences in the width of the mid-IR resonance. The similar line shape is indicative of a similar origin of the mid-IR resonance in both insulating and conducting samples (VB-to-IB optical excitations). The scaled  $\text{Ga}_{1-x}\text{Mn}_x\text{As}$  data include early IR results, with different growth procedures (rotated and nonrotated, postgrowth annealing, etc.) that imply variable levels of disorder, yet the qualitative features reveal only minimal dependence on the degree of disorder. These facts allow us to conclude that disorder is not playing a major role in the infrared response of  $\text{Ga}_{1-x}\text{Mn}_x\text{As}$ . Another result evident from Fig. 3 is the prominent Drude peak observed only in  $\text{Ga}_{1-x}\text{Be}_x\text{As}$  samples. Much weaker low-energy spectral weight is exhibited in Mn-doped samples, even those subjected to low-temperature annealing known to enhance the carrier density<sup>29</sup> (further discussion of low- $\omega$  analysis of Be and Mn-doped samples can be found in the Supplemental Material<sup>7</sup>). All these findings demonstrate the distinct nature of transport in films with magnetic Mn dopants.

The quantum defect method for band-to-acceptor transitions (black dashed curve in Fig. 3)<sup>14</sup> (see the Supplemental Material for model details<sup>7</sup>), as well as more complex calculations,<sup>30,31</sup> have been shown to successfully capture

key aspects of the mid-IR resonance in  $\text{Ga}_{1-x}\text{Mn}_x\text{As}$ . However, other explanations of the mid-IR resonance have been proposed,<sup>10</sup> and the microscopic justification of such “impurity band models” have been called into question.<sup>32</sup> Our systematic study showing the mid-IR resonance exists in the insulating regime, and persists with the same line form across the IMT up to the highest attainable doping, conclusively demonstrates impurity states dominate electronic dynamics in  $\text{Ga}_{1-x}\text{Mn}_x\text{As}$ , even in highly conductive samples.

Aspects of coexistence of the IB and metallicity are perhaps understandable very near the IMT, as in the case of the  $x = 9.5 \times 10^{-5}$  Be-doped sample. However, our results show that in the magnetically doped films, signatures of IB states remain, along with the coexistence of metallic and insulating trends, at least an order of magnitude in dopant concentration beyond that associated with the onset of conduction. Theoretical work has directly linked exchange coupling between Mn ions and valence holes to the persistence of the IB in  $\text{Ga}_{1-x}\text{Mn}_x\text{As}$ ,<sup>33,34</sup> further underscoring the pivotal role of magnetism in the electronic structure and optical phenomena of  $\text{Ga}_{1-x}\text{Mn}_x\text{As}$ . Because trivial clustering of multiple phases has been ruled

out in  $\text{Ga}_{1-x}\text{Mn}_x\text{As}$ ,<sup>35,36</sup> the duality between metallic and insulating trends appear to be an intrinsic attribute of the IMT in magnetically  $p$ -doped GaAs.<sup>37</sup> In view of the above duality, it may not be surprising that some properties of  $\text{Ga}_{1-x}\text{Mn}_x\text{As}$  can be explained from the standpoint of Bloch-like states.<sup>32,38,39</sup> However, many salient features of  $\text{Ga}_{1-x}\text{Mn}_x\text{As}$  cannot be understood in the context of conventional VB conduction, such as the spectral features and activated trends seen in Fig. 1, and require an emphasis on localization.<sup>30,31,40</sup> We speculate electronic correlations are likely to be vitally important in a conducting system at the borderline of localization, and note earmarks of such correlation effects have been identified in  $\text{Ga}_{1-x}\text{Mn}_x\text{As}$  tunneling spectra.<sup>36</sup> Though disorder plays a role, our experiments show that disorder alone is not sufficient to explain the radical differences between Be- and Mn-doped samples.

Work at UCSD is supported by the Office of Naval Research. Work at UCSB is supported by the Office of Naval Research and the National Science Foundation.

\*bchapler@physics.ucsd.edu

<sup>1</sup>J. M. D. Coey *et al.*, *Adv. Phys.* **48**, 167 (1999).

<sup>2</sup>K. S. Burch, D. D. Awschalom, and D. N. Basov, *J. Magn. Magn. Mater.* **320**, 3207 (2008).

<sup>3</sup>K. Sato *et al.*, *Rev. Mod. Phys.* **82**, 1633 (2010).

<sup>4</sup>R. C. Myers, B. L. Sheu, A. W. Jackson, A. C. Gossard, P. Schiffer, N. Samarth, and D. D. Awschalom, *Phys. Rev. B* **74**, 155203 (2006).

<sup>5</sup>S. Mack *et al.*, *Appl. Phys. Lett.* **92**, 192502 (2008).

<sup>6</sup>Y. Nagai and K. Nagasaka, *Infrared Phys. Technol.* **48**, 1 (2006).

<sup>7</sup>See Supplemental Material at <http://link.aps.org/supplemental/10.1103/PhysRevB.84.081203>.

<sup>8</sup>B. L. Sheu, R. C. Myers, J. M. Tang, N. Samarth, D. D. Awschalom, P. Schiffer, and M. E. Flatte, *Phys. Rev. Lett.* **99**, 227205 (2007).

<sup>9</sup>R. Moriya and H. Munekata, *J. Appl. Phys.* **93**, 4603 (2003).

<sup>10</sup>T. Jungwirth *et al.*, *Phys. Rev. B* **76**, 125206 (2007).

<sup>11</sup>J. Okabayashi, A. Kimura, O. Rader, T. Mizokawa, A. Fujimori, T. Hayashi, and M. Tanaka, *Phys. Rev. B* **64**, 125304 (2001).

<sup>12</sup>E. J. Singley, R. Kawakami, D. D. Awschalom, and D. N. Basov, *Phys. Rev. Lett.* **89**, 097203 (2002).

<sup>13</sup>K. S. Burch, D. B. Shrekenhamer, E. J. Singley, J. Stephens, B. L. Sheu, R. K. Kawakami, P. Schiffer, N. Samarth, D. D. Awschalom, and D. N. Basov, *Phys. Rev. Lett.* **97**, 087208 (2006).

<sup>14</sup>E. Kojima, J. B. Heroux, R. Shimano, Y. Hashimoto, S. Katsumoto, Y. Iye, and M. Kuwata-Gonokami, *Phys. Rev. B* **76**, 195323 (2007).

<sup>15</sup>K. Ando, H. Saito, K. C. Agarwal, M. C. Debnath, and V. Zayets, *Phys. Rev. Lett.* **100**, 067204 (2008).

<sup>16</sup>S. Ohya, I. Muneta, P. N. Hai, and M. Tanaka, *Phys. Rev. Lett.* **104**, 167204 (2010).

<sup>17</sup>M. A. Mayer, P. R. Stone, N. Miller, H. M. Smith, O. D. Dubon, E. E. Haller, K. M. Yu, W. Walukiewicz, X. Liu, and J. K. Furdyna, *Phys. Rev. B* **81**, 045205 (2010).

<sup>18</sup>V. F. Sapega, M. Moreno, M. Ramsteiner, L. Daweritz, and K. Ploog, *Phys. Rev. Lett.* **94**, 137401 (2005).

<sup>19</sup>L. P. Rokhinson, Y. Lyanda-Geller, Z. Ge, S. Shen, Liu, X. Liu, M. Dobrowolska, and J. K. Furdyna, *Phys. Rev. B* **76**, 161201(R) (2007).

<sup>20</sup>Y. Okimoto, T. Katsufuji, T. Ishikawa, A. Urushibara, T. Arima, and Y. Tokura, *Phys. Rev. Lett.* **75**, 109 (1995).

<sup>21</sup>K. Hirakawa, *Physica E* **10**, 215 (2001).

<sup>22</sup>D. N. Basov *et al.*, *Rev. Mod. Phys.* **83**, 471 (2011).

<sup>23</sup>D. Romero, S. Liu, H. D. Drew, and K. Ploog, *Phys. Rev. B* **42**, 3179 (1990).

<sup>24</sup>A. Gaymann, H. P. Geserich, and H. v. Lohneysen, *Phys. Rev. B* **52**, 16486 (1995).

<sup>25</sup>Choice in cutoff excludes contributions from excitations into the GaAs conduction band, and facilitates direct comparison with other studies in the literature (Refs. [13] and [26]).

<sup>26</sup>J. Sinova, T. Jungwirth, S. R. Eric Yang, J. Kucera, and A. H. MacDonald, *Phys. Rev. B* **66**, 041202 (2002).

<sup>27</sup>W. Songprakob *et al.*, *J. Appl. Phys.* **91**, 171 (2002).

<sup>28</sup>R. Braunstein and E. O. Kane, *J. Phys. Chem. Solids* **23**, 1423 (1962).

<sup>29</sup>K. M. Yu, W. Walukiewicz, T. Wojtowicz, I. Kuryliszyn, X. Liu, Y. Sasaki, and J. K. Furdyna, *Phys. Rev. B* **65**, 201303 (2002).

<sup>30</sup>C. P. Moca, G. Zarand, and M. Berciu, *Phys. Rev. B* **80**, 165202 (2009).

<sup>31</sup>G. Bouzerar and R. Bouzerar, *New J. Phys.* **13**, 023002 (2011).

<sup>32</sup>J. Mašek *et al.*, *Phys. Rev. Lett.* **105**, 227202 (2010).

<sup>33</sup>A.-M. Nili *et al.*, e-print arXiv:1007.4609V1.

<sup>34</sup>A. Chattopadhyay, S. DasSarma, and A. J. Millis, *Phys. Rev. Lett.* **87**, 227202 (2001).

<sup>35</sup>S. R. Dunsiger *et al.*, *Nat. Mater.* **9**, 299 (2010).

<sup>36</sup>A. Richardella *et al.*, *Science* **327**, 665 (2010).

<sup>37</sup>V. F. Sapega, N. I. Sablina, I. E. Panaiotti, N. S. Averkiev, and K. H. Ploog, *Phys. Rev. B* **80**, 041202(R) (2009).

<sup>38</sup>T. Jungwirth *et al.*, *Rev. Mod. Phys.* **78**, 809 (2006).

<sup>39</sup>T. Dietl *et al.*, *Science* **287**, 1019 (2000).

<sup>40</sup>R. Bouzerar and G. Bouzerar, *Europhys. Lett.* **92**, 47006 (2010).